

# Lack of Association of a Spontaneous Mutation of the *Chrm2* Gene with Behavioral and Physiologic Phenotypic Differences in Inbred Mice

Ming Ding,<sup>1</sup> Jennifer Arnold,<sup>1</sup> Jeremy Turner,<sup>2,3</sup> Vickram Ramkumar,<sup>1</sup> Larry F Hughes,<sup>2</sup> Rita A Trammell,<sup>4</sup> and Linda A Toth<sup>1,2\*</sup>

The nucleotide substitution C797T in the *Chrm2* gene causes substitution of leucine for proline at position 266 (P266L) of the CHRM2 protein. Because *Chrm2* codes for the type 2 muscarinic receptor, this mutation could influence physiologic and behavioral phenotypes of mice. *Chrm2* mRNA was not differentially expressed in 2 brain regions with high cholinergic innervation in a mouse strain that does (BALB/cByJ) or does not (C57BL/6J) have the mutation. In addition, strains of mice with and without the C797T point mutation in *Chrm2* did not differ significantly in muscarinic binding properties. Variation across strains was detected in terms of acoustic startle, prepulse inhibition, and the physiologic effects of the muscarinic agonist oxotremorine. However, interstrain differences in these measures did not correlate with the presence of the mutation. Although we were unable to associate a measurable phenotype with the *Chrm2* mutation, assessment of the mutation on other genetic backgrounds or in the context of other traits might reveal differential effects. Therefore, despite our negative findings, evaluation of characteristics that involve muscarinic function should be undertaken with caution when comparing mice with different alleles of the *Chrm2* gene.

**Abbreviations:** M2R, type 2 muscarinic receptor; NMS, N-methylscopolamine; OXO, oxotremorine; PPI, prepulse inhibition; RI, recombinant inbred.

Acetylcholine, a crucial neurotransmitter in both the central and peripheral nervous systems, acts through 2 major types of receptors: muscarinic and nicotinic. Muscarinic acetylcholine receptors are members of the superfamily of G protein-coupled receptors.<sup>17</sup> mRNA and protein for the type 2 muscarinic receptor (M2) are present in many peripheral and central sites in the nervous system and peripheral target organs. M2R mediates a complex combination of postsynaptic and presynaptic events in noncholinergic and cholinergic neurons, respectively.<sup>9</sup>

The M2R is encoded by the gene *Chrm2*. The proline at position 266 and surrounding residues of the *Chrm2* gene are relatively conserved across several species, including human, rat, mouse, and swine (<http://www.ncbi.nlm.nih.gov/>). However, a nucleotide substitution (C797T) has been identified in several strains of inbred mice (Mouse Genome Informatics SNP query for *Chrm2*; <http://www.informatics.jax.org/searches>). This nucleotide substitution results in an amino acid substitution, P266L, in the protein. Proline is the only amino acid that contains a secondary amino group and forms tertiary peptide bonds. Because of this attribute, substitution of leucine for proline could cause allosteric alterations in proteins, with potential structural or functional consequences.

Allosteric modulation is a recognized regulatory mechanism of muscarinic receptors.<sup>17,21</sup> For example, introduction of a point mutation (Asn to Tyr) at position 410 (the junction of trans-

membrane domain 6 and the 3rd intracellular loop) of the human M2R generated a constitutively active receptor with altered receptor–G-protein coupling in response to agonist administration.<sup>23</sup> Single-nucleotide polymorphisms in the human *Chrm2* gene are implicated in responses to visual stimuli requiring attention, working memory, and response selection.<sup>8,15,16</sup> In addition, a common *Chrm2* polymorphism has been associated with major depression in women in some studies<sup>6,35</sup> but not others.<sup>5</sup> Furthermore, *Chrm2* has been implicated in nicotine addiction; *Chrm2* single-nucleotide polymorphisms may be associated with the general possibility of becoming addicted, personality traits that predispose the person to becoming addicted, or altered regulation of cholinergic systems that affect the smoker's response to nicotine and its addictive properties.<sup>22</sup>

These reports suggest that mouse strains that bear the *Chrm2* mutation, as compared with strains that do not, potentially provide a unique model for exploring mechanisms by which *Chrm2* variants may affect cholinergic mechanisms and associated physiologic processes in both brain and the periphery. We report here on studies conducted to determine whether the C797T *Chrm2* mutation confers a detectable phenotypic difference in M2R-related processes in mice.

## Materials and Methods

**Approval of animal use.** All animal experimentation presented here was approved in advance by the Laboratory Animal Care and Use Committee of the Southern Illinois University School of Medicine.

**Mice.** Adult male C57BL/6J, BALB/cByJ, and CXB recombinant inbred (RI) mice were obtained from the Jackson Laboratory

Received: 05 Dec 2008. Revision requested: 08 Dec 2008. Accepted: 15 Jun 2010.  
Departments of <sup>1</sup>Pharmacology, <sup>2</sup>Surgery, and <sup>3</sup>Medicine, Southern Illinois University School of Medicine, Springfield, Illinois; <sup>4</sup>Department of Psychology, Illinois College Jacksonville, Illinois.

\*Corresponding author. Email: ltoth@siu.edu

(Bar Harbor, ME). All mice were free of known infections with common rodent viral, bacterial and parasitic agents, as monitored using monthly testing of sentinel mice housed in the same room. Mice used in these experiments were housed in groups of 5 on hardwood bedding, with food (Purina Laboratory Chow, PMI Nutrition International, St Louis, MO) and water available ad libitum. The animal holding room was maintained on a 12:12-h light:dark cycle at  $22 \pm 1$  °C with 35% to 50% relative humidity. Routine noise exposure, as occurs in association with standard husbandry practices, was not controlled. All mice used in this study were euthanized by cervical dislocation under isoflurane anesthesia.

**Acoustic startle, acoustic gap detection, and prepulse inhibition (PPI) of startle.** Assessment of acoustic startle, acoustic gap detection, and PPI of startle was conducted by using startle reflex hardware and software (Kinder Scientific, Poway, CA) customized for this application by the manufacturer. Testing was conducted with background noise and startle stimuli presented through a speaker located in the ceiling of the testing chamber, 15 cm above the mouse's head. The floor of the chamber was attached to a piezo transducer and provided a measure of startle force (calibrated in Newtons) applied to the floor. A clear polycarbonate mouse holder, with holes to permit sound passage, was suspended above the floor, allowing the mouse to turn around freely while minimizing excessive movement. An adjustable-height roof was set to a level that prevented rearing, to minimize variability in the startle response. Test stimuli were calibrated by using a cloth model mouse and a 1/2-in. free-field microphone (model 41941A, Bruel and Kjaer, Nærum, Denmark) connected to a conditioning amplifier (Nexus type 2690, Bruel & Kjaer, Nærum, Denmark) and an analog-to-digital board (USB6251, National Instruments, Austin, TX). Custom sound analysis software (written in LabView [National Instruments]) was used to visualize and calibrate the acoustic signals.

Behavioral testing sessions consisted of placing a mouse in the test chamber, followed by a 2-min acclimation period to allow adjustment to the novel environment. At that point, 2 exposures to an abrupt startle-eliciting noise burst (110 dB SPL, 20 ms in duration) were presented to habituate the mouse's startle response and improve the stability of baseline measurements. Data from these 2 initial trials were not used in the analysis. The remainder of the 20- to 25-min session consisted of stimulus trials presented at a rate of 4 stimuli per minute (the intertrial interval varied and averaged 15 s between trials). During the session, C57BL/6J and BALB/cByJ mice were exposed to intermixed startle-only trials and trials in which the startle stimulus was preceded by either a silent period in the otherwise continuous 60-dB SPL background sound (gap detection testing) or a prepulse stimulus of either 5 or 10 dB SPL above the 60-dB background (PPI testing). PPI testing for the RI strains was conducted by using prepulse stimuli of 30, 45, and 60 dB SPL with a quiet background (instead of 5 or 10 dB above background), to detect deficits in PPI due to hearing loss rather than sensory gating deficits. The beginning of the gap and prepulse stimuli always occurred 100 ms before the startle stimulus, and the stimuli were 50 ms in duration and shaped with a 0.1-ms rise-fall gate. These procedures provided sensitive measures of hearing function and sensory gating processes in rodents. Previous work indicates that such testing does not cause temporary or permanent elevations in hearing thresholds in mice.<sup>29,37,38,40</sup>

**Physiologic responses to oxotremorine (OXO).** Mice were injected with the muscarinic agonist OXO and then tested for the following: heart rate, body temperature, tremor, salivation, and response to painful stimuli. For quantification of body temperature, mice were implanted with a subcutaneous transponder (BioMedic Data Systems, Seaford, DE) that permitted rapid and noninvasive measurement of temperature by use of a wand-type scanner. Transponders were implanted by use of a trochar and isoflurane anesthesia a minimum of 7 d prior to experimental use. All testing was conducted during the light phase between approximately 1000 and 1400. On the day of testing, basal temperatures were measured by using the wand scanner. Mice then were injected intraperitoneally with vehicle (pyrogen-free saline) or 1 of 3 doses (0.1, 0.2, or 0.3 mg/kg) of OXO (Sigma, St Louis, MO). Physiologic variables (tremor, salivation, core temperature, and response to pain) were assessed at 30 min after injection. First, temperature was measured by using the wand scanner. Next, mice were placed individually on the plate of a balance, and tremor was assessed according to the following scale: 0, no tremor; 1, intermittent head and body tremor; or 2, nearly continuous whole-body tremor. At this time, mice also were assessed for visible salivation as follows: 0, none; 1, mild; 2, moderate; and 3, severe. Mice then were placed in a plastic restrainer with the tail exposed. The tail was immersed in a 55 °C water bath, and withdrawal latency was measured, with a 15-s maximal withdrawal time permitted to avoid tissue damage. Increased latency to withdrawal indicates OXO-induced analgesia, which is absent in mice that lack M2R.<sup>36</sup> Finally, mice were placed on a 55 °C hot plate. Response latency to lick the fore or hind paws was measured, again with a 15-s maximal response time permitted. Mice received only 1 dose of OXO or vehicle and were euthanized after the evaluation was completed.

A second series of mice that included several CXB RI strains was used to evaluate the effects of OXO (0.1 mg/kg) on temperature, heart rate, salivation, and tremor. Baseline temperatures and heart rates were measured immediately after light onset approximately 1 wk before OXO administration. Basal temperatures were measured by using the wand scanner, as described earlier. Heart rates were measured under methoxyflurane-induced anesthesia sufficient to prevent spontaneous movement. Electrocardiograms were obtained by positioning microalligator clip leads on the skin along both sides of the rib cage. The electrocardiogram signals were differentially amplified, bandpass-filtered (0.1 to 100 Hz), and displayed by using a Grass polygraph recorder (model 7, Astromed, West Warwick, RI). Samples of heart rate were obtained for a minimum of 10 s for each mouse. These procedures produced records with distinct QRS waveforms, which then were counted manually to determine heart rate. OXO injections were made immediately after light onset, with temperature and heart rate measured 30 min thereafter. Mice also were assessed for tremor and salivation at that time, as described earlier.

**RT-PCR analysis in hypothalamus and basal forebrain.** *Chrm2* transcription was measured in basal forebrain and hypothalamus of healthy mice and mice infected with influenza virus. Influenza inoculation of mice under light methoxyflurane anesthesia was performed immediately after light onset and comprised intranasal application of 25 or 50  $\mu$ L allantoic fluid containing approximately 1,000 hemagglutinating units of strain A/HKx31 influenza virus.<sup>32,33</sup>

Mice were euthanized for tissue collection at 30 h after inoculation. This postinoculation time point is associated with differences in sleep that have been linked to the quantitative trait locus *Srilp*, which incorporates *Chrm2*.<sup>34</sup> Hypothalamus was removed based on visual localization from the ventral surface of the brain. The brain then was sectioned by using 2 coronal cuts, one at the level of the optic chiasm, and the other about 1 mm rostral to the optic chiasm (approximately 0.014 mm anterior to and 0.34 mm posterior to bregma, respectively).<sup>24</sup> Basal forebrain was removed from the slice according to the visual landmarks of the anterior commissure, third ventricle, striatum, and olfactory tubercle. For PCR experiments, tissues from 2 to 5 mice were pooled for analysis, and 4 to 5 independent replications were performed.

Infection was verified for all mice by measuring pulmonary viral titers using a plaque formation assay in which monolayers of Madin–Darby canine kidney fibroblasts were incubated with serial 10-fold dilutions of lung homogenate. The tissue samples used in this study had been assessed previously for expression of various genes (*Temt/Imnt*, *Ptgds*, and *Lcn2*). Influenza titers measured in lung at 30 h after infection were  $29 \pm 5$  pfu for BALB/cByJ mice ( $n = 44$ ) and  $29 \pm 7$  pfu for C57BL/6J mice ( $n = 36$ ; the high numbers of samples are due to individual measurements of titers in lungs of all mice included in pooled samples).

When collected for RT-PCR, tissues were placed in RNALater (Ambion, Austin, TX) immediately after dissection. Total RNA was extracted by using TRIzol (Invitrogen, Carlsbad, CA) and was digested with DNase I (Invitrogen). cDNA was synthesized from total RNA by using Superscript (Invitrogen). Expression of *Chrm2* was estimated by RT-PCR by using a primer pair designed according to the sequence of murine *Chrm2* (NCBI sequence XM\_145245). The sense primer was 5' CAC TGG GAG AAG TGG AGG AG 3' (nucleotides 137 to 156), and the antisense primer was 5' CCC AGA GGA TGA AGG AAA GA 3' (nucleotides 918 to 937). The glyceraldehyde-3-phosphate dehydrogenase gene (*Gapdh*, BC083149) was used as reference or 'housekeeping' gene; the sense primer was 5' AAC GAC CCC TTC ATT GAC 3' (nucleotides 130 to 147), and the antisense primer was 5' GAA GAC ACC AGT AGA CTC CAC 3' (nucleotides 316 to 336). The PCR mix (10  $\mu$ L) consisted of 1  $\mu$ L cDNA, 1  $\mu$ L each 10-pmol primer, reaction buffer, 200  $\mu$ M each dNTP, 2.5 mM  $MgCl_2$ , and 0.5 U *Taq* polymerase (Invitrogen). Reactions were carried out in a thermocycler (5 min at 94 °C, followed by 35 cycles of 1 min at 94 °C, 1 min at 58 °C, and 2 min at 72 °C). PCR products were separated electrophoretically on agarose gels and visualized with ethidium bromide under UV illumination.

***Chrm2* sequence and genotype analysis.** cDNA was synthesized from the lungs of C57BL/6J and BALB/cByJ mice. Three primer pairs were designed according to the sequence of murine *Chrm2* gene (XM\_145245). The PCR mix (10  $\mu$ L) consisted of 1  $\mu$ L of DNA, 1  $\mu$ L of each 10-pmol primer, reaction buffer, 200  $\mu$ M each dNTP, 2.5 mM  $MgCl_2$ , and 0.5 U *Taq* polymerase (Invitrogen). Reactions were carried out in a thermocycler (5 min at 94 °C, followed by 35 cycles of 1 min at 94 °C, 1 min at 58 °C, and 2 min at 72 °C). PCR products were purified from the agarose gel by using a GeneClean II Kit (Q.BIO Gene, Carlsbad, CA). The University of Iowa DNA Core Facility (Iowa City, IA) performed sequence analysis by using the BigDye Terminator version 3.1 Cycle Sequencing Kit (ABI Applied Biosystems, Foster City, CA) and an Prism 3100 Genetic Analyzer (ABI Applied Biosystems). Polymorphisms were identified by comparing sequences from

C57BL/6J and BALB/cByJ mice by using GeneRunner software (Hastings Software; www.generunner.net).

For genotyping, genomic DNA was extracted from the livers of C57BL/6J and BALB/cByJ mice. *Chrm2* primer pairs were designed according to the sequence of murine *Chrm2* (XM\_145245). The sense primer was 5' ACA AAA ATG GCA GGC ATG AT 3' (nucleotides 880 to 899), and the antisense primer was 5' TGG AGT CGT TGG AGC TTT CT 3' (nucleotides 1311 to 1330). PCR was performed as described earlier. PCR products were digested by using *Sac II* (New England Biolabs, Ipswich, MA) in reaction buffer IV. Reaction mixtures were separated by electrophoresis on 2.5% agarose gel and visualized with ethidium bromide under UV illumination.

**Receptor binding.** Competition curves for OXO were performed by using heart homogenates, with [<sup>3</sup>H]-N-methylscopolamine (NMS) as the radioligand. Muscarine and OXO are both full muscarinic receptor agonists, with affinity for both M1 and M2 subtypes. OXO was used as the primary agonist to permit comparison with the in vivo studies of agonist effects. In heart, M2 is the major muscarinic receptor.<sup>31</sup> Therefore, [<sup>3</sup>H]NMS should compete preferentially against M2-bound ligands in that tissue.

Mouse heart was homogenized on ice in 50 mM  $Na^+/K^+$  phosphate buffer (pH 7.3) for 30 s. The homogenates were centrifuged at  $5000 \times g$  for 15 min, and the resulting supernatant was centrifuged at  $30,000 \times g$  for 30 min. The final pellet was suspended in 50 mM  $Na^+/K^+$  phosphate buffer (pH 7.3) at a working concentration (w/v) of 5%. Supernatant (0.15 mg protein) was incubated in duplicate for 90 min at room temperature with 1 nM [<sup>3</sup>H]NMS in 1 mL 50 mM  $Na^+/K^+$  phosphate buffer (pH 7.3). Assays were terminated by vacuum filtration by using a cell harvester (Brandel, Gaithersburg, MD). Filters (Whatman GF/B, Brandel, Gaithersburg, MD) were washed 3 times with ice-cold isotonic saline. The radioactivity on each filter was quantified by using a liquid scintillation counter (model LS5801, Beckman Instruments, Fullerton, CA).

To test the ability of oxotremorine to compete for [<sup>3</sup>H]NMS binding sites, tissue was incubated without or with 10  $\mu$ M GTP $\gamma$ S prior to performing oxotremorine competition curves. Competition curves were analyzed by using Graph Pad Prism 4.0 software (GraphPad Software, San Diego, CA) with a one-site fit.

**Statistical analysis.** Data files generated during the experiments were imported to Excel spreadsheets (Microsoft, Redmond, WA) and assessed for integrity and distributional characteristics. Descriptive statistics and graphic depictions were used to determine whether transformations were necessary to meet the assumptions of the inferential statistical procedures used. Statistical procedures were implemented with SPSS 14.0 (SPSS, Chicago, IL) and NCSS 2007 (NCSS, Kaysville, UT).

ANOVA was the primary method for examining the relationship between means related to treatment conditions. The analyses included main effects and all interactions. Factorial and one-way ANOVA and estimation of simple effects were used for measurements made at a single point in time. Longitudinal measurements used mixed ANOVA with repeated measurements. If data did not meet assumptions concerning sphericity, the Greenhouse–Geisser correction was used. When an independent variable had more than 2 levels, or if an interaction was detected between 2 or more variables, tests were conducted subsequent to the overall ANOVA to determine specifically which pairs of means differed from each other. Comparisons were limited to those specified in advance.

For planned comparisons in which the numbers of comparisons did not exceed the degrees of freedom, the omnibus test was not conducted, and planned comparisons were performed without adjustment of the  $\alpha$  level. If the number of planned comparisons exceeded the available degrees of freedom, Bonferroni adjustments were made. The Dunnett test was used to compare the mean of a single control group with means of the other groups. The Scheffé procedure was used for post hoc comparisons. A value of  $P < 0.05$  was considered to indicate a statistically significant effect.

Measures of association between 2 discrete variables were analyzed by using the  $\chi^2$  test. If expected frequencies were too small for a valid  $\chi^2$  test, the Fisher exact test was used.

## Results

**Identification and expression of *Chrm2* mutation.** *Chrm2* sequence analysis was performed by using cDNA synthesized from the lungs of C57BL/6J and BALB/cByJ mice. A C→T single nucleotide substitution was found at nucleotide 797 from the start codon in the *Chrm2* gene of BALB/cByJ mice. This substitution, C797T, results in an amino acid change from proline to leucine at position 266 (P266L) of the protein CHRM2. The P266L missense mutation is located in the third intracellular loop of the CHRM2 protein, between 2 M2R-binding regions.<sup>11</sup> P266 and the surrounding residues of CHRM2 are relatively conserved across species, including human, rat, mouse, and swine (Figure 1 A).

This point mutation was confirmed by using the restriction enzyme *Sac II* to digest the 451-bp PCR product that incorporates the substitution. The C797T nucleotide substitution in the *Chrm2* gene caused loss of a recognition site for the restriction enzyme *SacII*, such that the BALB/cByJ cDNA was resistant to *SacII* and remained as a 451-bp unit. In contrast, the PCR product from C7BL/6J mice was cleaved into the 2 expected fragments of 392 and 59 bp.

The C797T nucleotide substitution was used as a marker to genotype several inbred strains of mice, including the 13-strain CXB RI set (Figure 1 B). The resultant strain distribution pattern shows that the mutation is also present in A/J and DBA/2J mice and in some lines of the CXB RI set but not in C3H/HeJ mice. In addition, the mutation is present in mouse strains BALB/cJ, BALB/cAnNHsd, BALB/c01aHsd, BALB/cAnNCrI, BALB/cAnNTac, and AKR/J (data not shown).

To determine whether the mutation influenced gene expression in brain, hypothalamus and basal forebrain collected from uninfected and influenza-infected C57BL/6J and BALB/cByJ mice underwent RT-PCR analysis. The PCR product for *Chrm2* cDNA was clearly visible in both structures of uninfected and infected mice (Figure 1 C). Densitometry and normalization to *Gadph* product did not reveal significant differences in expression as a function of either mouse strain or health status.

**Effect of the P266L *Chrm2* mutation on M2R-related physiology and behavior. Responses to the muscarinic agonist OXO.** Administration of the muscarinic agonist OXO causes hypothermia, tremor, and analgesia in genetically intact mice but not in mice that lack *Chrm2*.<sup>36</sup> To test whether M2R-related responses differ between strains that do or do not have a P266L mutation of *Chrm2*, C57BL/6J and BALB/cByJ mice were treated with various doses of OXO, and physiologic signs of M2R activation (tremor, salivation, pain perception, and core temperature) were evaluated.

At 30 min after injection, OXO induced significant dose-related hypothermia ( $P = 0.015$ ), prolongation of reaction time in the hot water withdrawal and hot plate reaction tests ( $P < 0.001$ ), and an increase in the proportion of mice showing tremor and salivation ( $P < 0.001$ ). However, these effects were not significantly influenced by mouse strain (Figure 2).

A second study evaluated heart rate, core temperature, and the severity of tremor and salivation at 30 min after administration of 0.1 mg/mg OXO to C57BL/6J, BALB/cByJ, and select strains of CXB RI mice (Figure 3). OXO administration induced significant strain-dependent variation in bradycardia ( $P = 0.002$ ), hypothermia ( $P = 0.006$ ), tremor severity ( $P < 0.0001$ ), and salivation severity ( $P = 0.003$ ). However, these variations were not correlated with the presence or absence of the *Chrm2* mutation (Table 1).

**Startle response and PPI of startle.** Two studies were performed to evaluate behavioral responses to acoustic stimuli: startle response and PPI of startle. The first study compared C57BL/6J and BALB/cByJ mice. Basal activity levels (that is, force applied to the sensing plate with no startle stimulus presented) of the 2 strains were similar, suggesting similar levels of ambulation and grooming. In the presence of constant background noise, startle amplitudes (measured in terms of force) were significantly larger in BALB/cByJ mice ( $1.37 \pm 0.22$  Newtons) than in C57BL/6J mice ( $0.66 \pm 0.11$  Newtons;  $n = 10$  per strain;  $P = 0.009$ ). In terms of gap detection, neither strain reliably detected gaps of 10 ms or lower, C57BL/6J mice detected 15-ms gaps, and both strains detected 50-ms gaps, although C57BL/6J were more reliable (Figure 4).

Collapsing data over all gap durations revealed no significant difference in overall gap detection between the 2 strains, given that the 2-way ANOVA (gap duration  $\times$  strain) was not significant ( $P = 0.943$ ). However, the main effect for strain revealed a trend ( $P = 0.092$ ) for better gap detection in C57BL/6J mice. Follow-up *t* tests revealed significant differences in gap detection in C57BL/6J and BALB/cByJ mice at gaps of both 15 ms ( $P = 0.047$ ) and 50 ms ( $P = 0.006$ ). Both strains showed similar, modest PPI in response to a 5-dB prepulse over background, with no difference between strains ( $P = 0.939$ ; Figure 4). However, C57BL/6J mice had a more robust PPI to a 10-dB prepulse above background; this response was significantly ( $P = 0.002$ ) greater than that of BALB/cByJ mice (Figure 4).

The second study compared the responses of 4 strains of CXB RI mice in a quiet background. Startle amplitude was significantly ( $P = 0.002$ ) different across RI strains (Figure 5). Follow-up Scheffe tests for multiple comparisons revealed significant differences between CXB3 and CXB6 ( $P = 0.019$ ) and CXB6 and CXB9 ( $P = 0.018$ ) mice. Trends suggestive of differences emerged when CXB3 and CXB12 ( $P = 0.084$ ) and CXB9 and CXB12 ( $P = 0.080$ ) mice were compared.

In addition, RI strains were tested for PPI by using stimuli of 30, 45, and 60 dB in a quiet background, rather than the 5 or 10 dB above a 60-dB background that was used when testing C57BL/6J and BALB/cByJ mice. This modification allows more sensitive determination of whether differences in PPI were due to hearing loss or general deficits in sensory gating. PPI varied across the RI strains (significant main effect for strain,  $P = 0.05$ ; Figure 5). Follow-up Scheffe tests performed across strains revealed a marginally significant ( $P = 0.054$ ) difference when comparing CXB6 and CXB9 mice. In addition, the significant ( $P = 0.002$ ) strain  $\times$  PPI intensity interaction suggested that the differences across strains

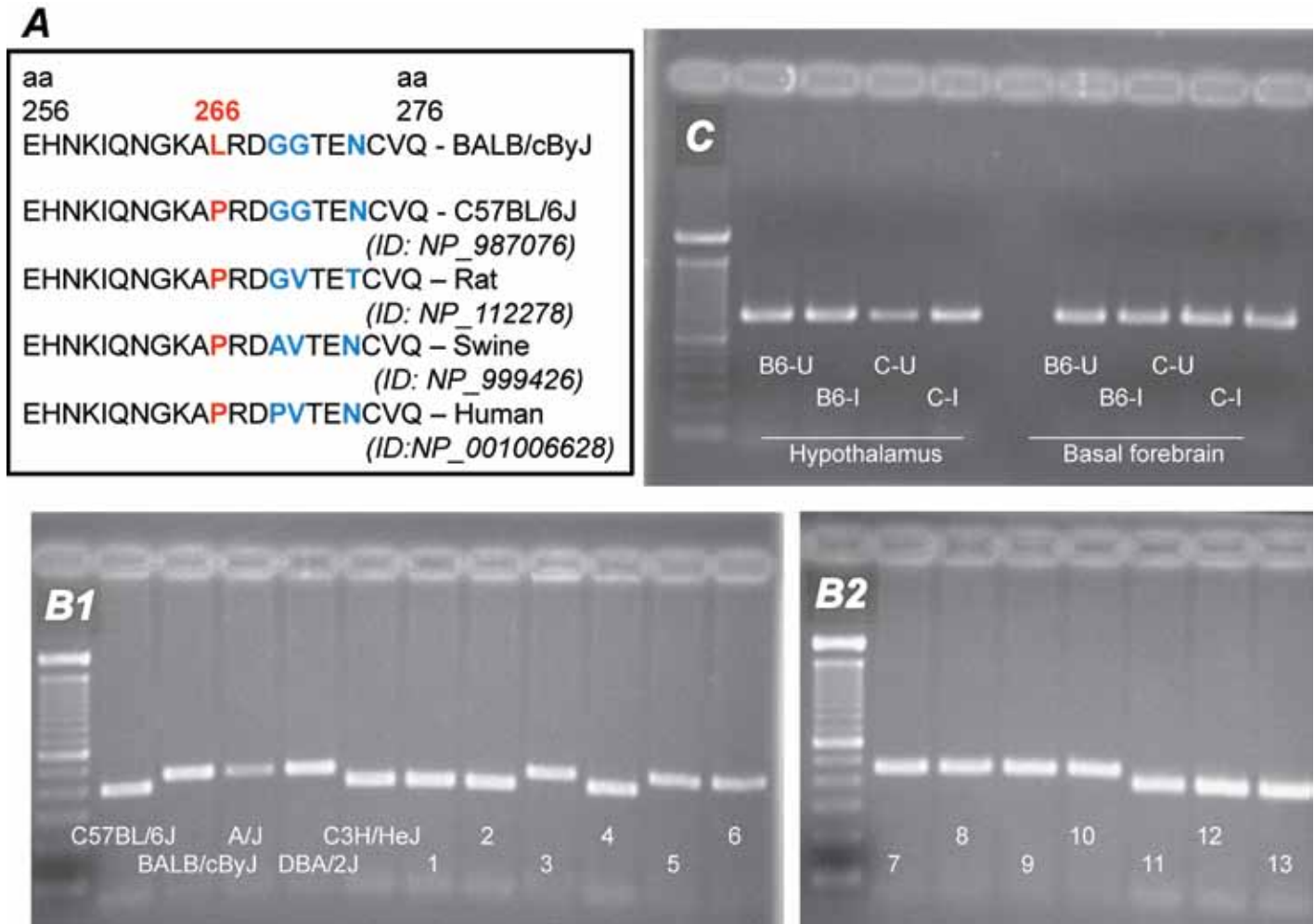


**Figure 1.** *Chrm2* genotype and expression in inbred mouse strains. (A) Species and mouse strain comparisons of the amino acids surrounding P266L in CHRM2 (from <http://www.ncbi.nlm.nih.gov/>). An ID number is not available for BALB/cByJ mice, as this is the first identification of this sequence and it is not yet in the NCBI database. (B) The *Sac* II restriction enzyme and cDNA products of PCR amplification were used to create a marker for genotyping. The first lane on each gel represents a molecular weight ladder. The BALB/cByJ allele, which is resistant to the enzyme, is visible as a 451-bp band. The C57BL/6J allele is cleaved by the enzyme, resulting in a 392-bp fragment and a 59-base pair fragment that, due to its low weight, is not visible on the gel. Numbers 1 through 13 denote CXB recombinant inbred strains. The C57BL/6J allele is shared by strains C3H/HeJ and CXB strains 1, 2, 4, 11, 12, and 13. The BALB/cByJ allele is shared by strains A/J, DBA/2J, and CXB strains 3, 5, 6, 7, 8, 9, and 10. (C) Hypothalamus and basal forebrain were collected at 30 h after inoculation of mice with either uninfected allantoic fluid or allantoic fluid that contained influenza virus for measurement of *Chrm2* mRNA. U, uninfected; I, influenza-infected; B6, C57BL/6J; C, BALB/cByJ.

were dependent on the intensity of the prepulse stimulus used (Figure 5).

**Receptor binding and signal transduction.** The inhibitory potencies ( $IC_{50}$ ) of OXO for competing at [ $^3H$ ]NMS binding sites were statistically similar for C57BL/6J and BALB/cByJ mice ( $0.44 \pm 0.18$  and  $0.47 \pm 0.05$   $\mu$ M, respectively;  $n = 4$ ; data not shown).

A characteristic of G-protein-coupled receptors is the ability of GTP $\gamma$ S to shift competition curves.<sup>4</sup> Incubation of heart homogenates from BALB/cByJ mice with 10  $\mu$ M GTP $\gamma$ S shifted the OXO competition curve from  $IC_{50}$  values of  $0.39 \pm 0.04$   $\mu$ M to  $0.58 \pm 0.25$   $\mu$ M ( $n = 3$ ; Figure 6). Homogenates from C57BL/6J mice showed a shift in  $IC_{50}$  values in the presence of GTP $\gamma$ S from  $0.44 \pm 0.23$  to  $1.59 \pm 0.75$   $\mu$ M ( $n = 3$ ; Figure 6). These effects were not significantly different between the 2 strains.

## Discussion

Extensive characterization of mice with genetic deletion of each of the 5 muscarinic receptor subtypes has revealed that some physiologic and pharmacologic effects are elicited specifically by M2R stimulation in mice, as opposed to other muscarinic receptor subtypes.<sup>36</sup> Our data confirm the presence of a single-nucleotide polymorphism and an associated amino acid substitution in A/J and DBA/2J mice as compared with C57BL/6J mice (Mouse Genome Informatics SNP query for *Chrm2*; <http://www.informatics.jax.org/searches>) and further report the presence of this mutation in BALB/c-based strains, AKR/J and some CXB RI strains of mice, but not in C3H/HeJ mice and other CXB RI strains. The polymorphism that we detected potentially could influence various measures of receptor function, including affinity for agonists or antagonists, regulation of acetylcholine release in structures that receive cholinergic input, and efficacy

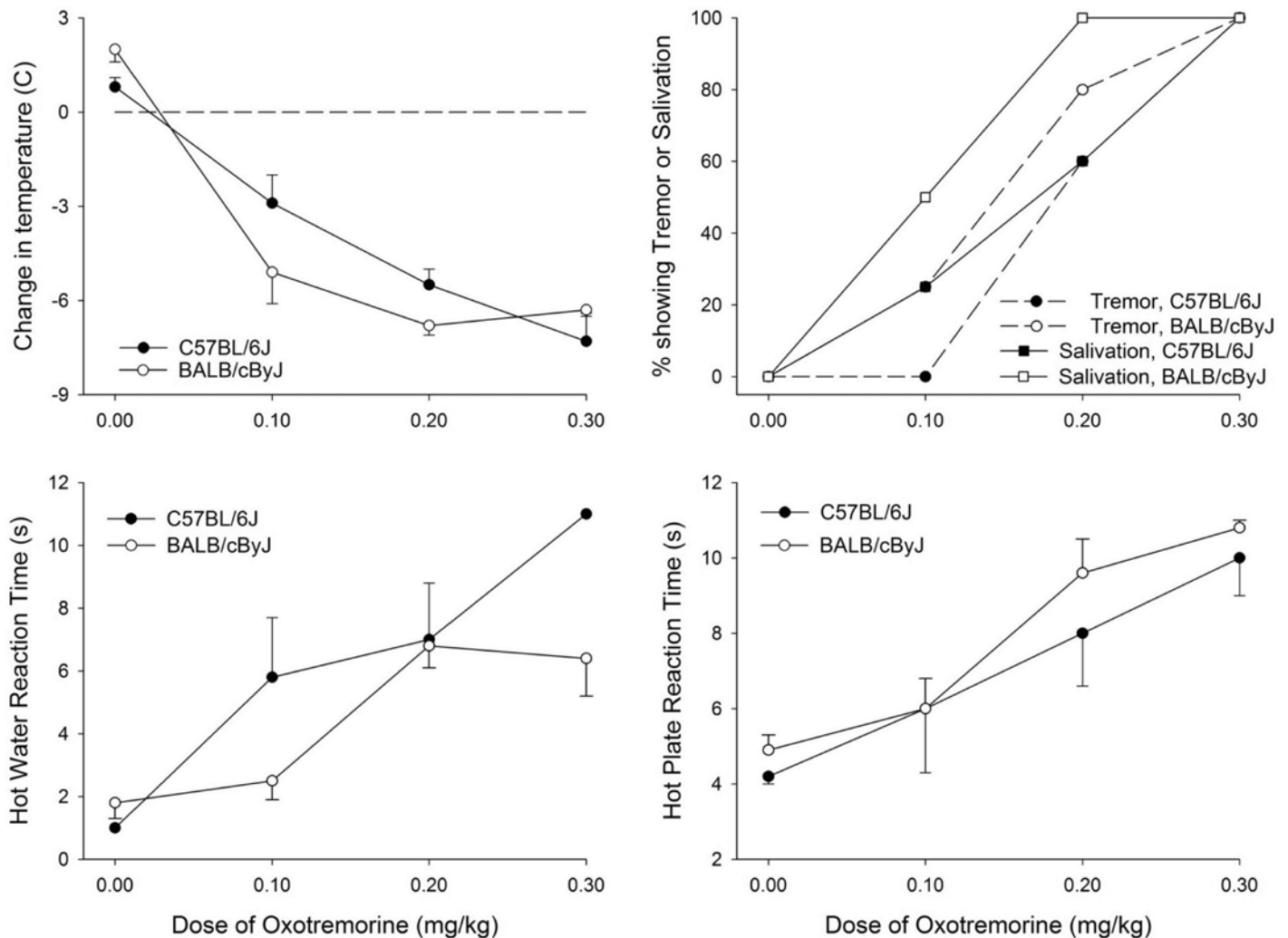


**Figure 2.** Physiologic and behavioral responses to oxotremorine in C57BL/6J and BALB/cByJ mice. Body temperature, salivation, tremor, and reactions to painful stimuli were assessed 30 min after intraperitoneal injection of vehicle (pyrogen-free saline) or 1 of 3 doses of OXO (0.1, 0.2, or 0.3 mg/kg;  $n = 8$  per strain at each dose). Tremor was assessed as: 0, no tremor; 1, intermittent head and body tremor; or 2, nearly continuous whole-body tremor. Salivation was assessed as: 0, none; 1, mild; 2, moderate; or 3, severe. For all panels, data are presented as mean  $\pm$  SEM (bars).

of signal transduction in mouse strains that bear the mutation. For example, BALB/c mice recently were reported to lack M2R-mediated cholinergic airway tone,<sup>18</sup> and airway smooth muscle tone is heavily modulated by M2R.<sup>13,27,39</sup> In humans, a common *Chrm2* polymorphism has been associated with poor response to bronchodilators in asthmatic patients<sup>30</sup> and poor outcomes after acute myocardial infarction.<sup>10</sup>

However, despite these relationships, we detected no difference between C57BL/6J and BALB/cByJ mice in several types of assessments that are relevant to M2R function. First, these strains showed no differences in competition of OXO at [<sup>3</sup>H]NMS binding sites in heart homogenate or in a shift in the OXO competition curve in the presence of GTP $\gamma$ S. Second, *Chrm2* transcription in basal forebrain and hypothalamus of these strains was not influenced by genotype and/or health status (that is, influenza infection). However, measuring expression of *Chrm2* at the cDNA level by using 35 cycles, as we did, is not quantitative and only confirms presence or absence of the transcript. The assessment of these brain areas and influenza infection was undertaken be-

cause basal forebrain and hypothalamus are acetylcholine-rich regions that high levels of M2R and are associated with sleep, arousal, and temperature control during states of both health and illness.<sup>9,19,28</sup>

In addition, C57BL/6J and BALB/cByJ mice differ in their somnogenic and immunologic responses to influenza infection,<sup>7,33</sup> leading us to speculate that the *Chrm2* polymorphism could have greater physiologic effect during illness. Third, the 2 strains of mice responded similarly in terms of hypothermia, tremor, salivation, and analgesia to in vivo administration of OXO. Although these responses to OXO are impaired in mice that lack *Chrm2* but not in mice that lack genes for other muscarinic receptors,<sup>36</sup> we found no evidence that the *Chrm2* mutation was associated with modification of these effects.

We were also unable to demonstrate a relationship between the *Chrm2* mutation and acoustic startle and PPI. Startle and PPI are dissociable traits. For example, muscarinic agonists can inhibit startle without affecting PPI.<sup>14</sup> The neuronal circuits that mediate startle and PPI share anatomic components, although the PPI

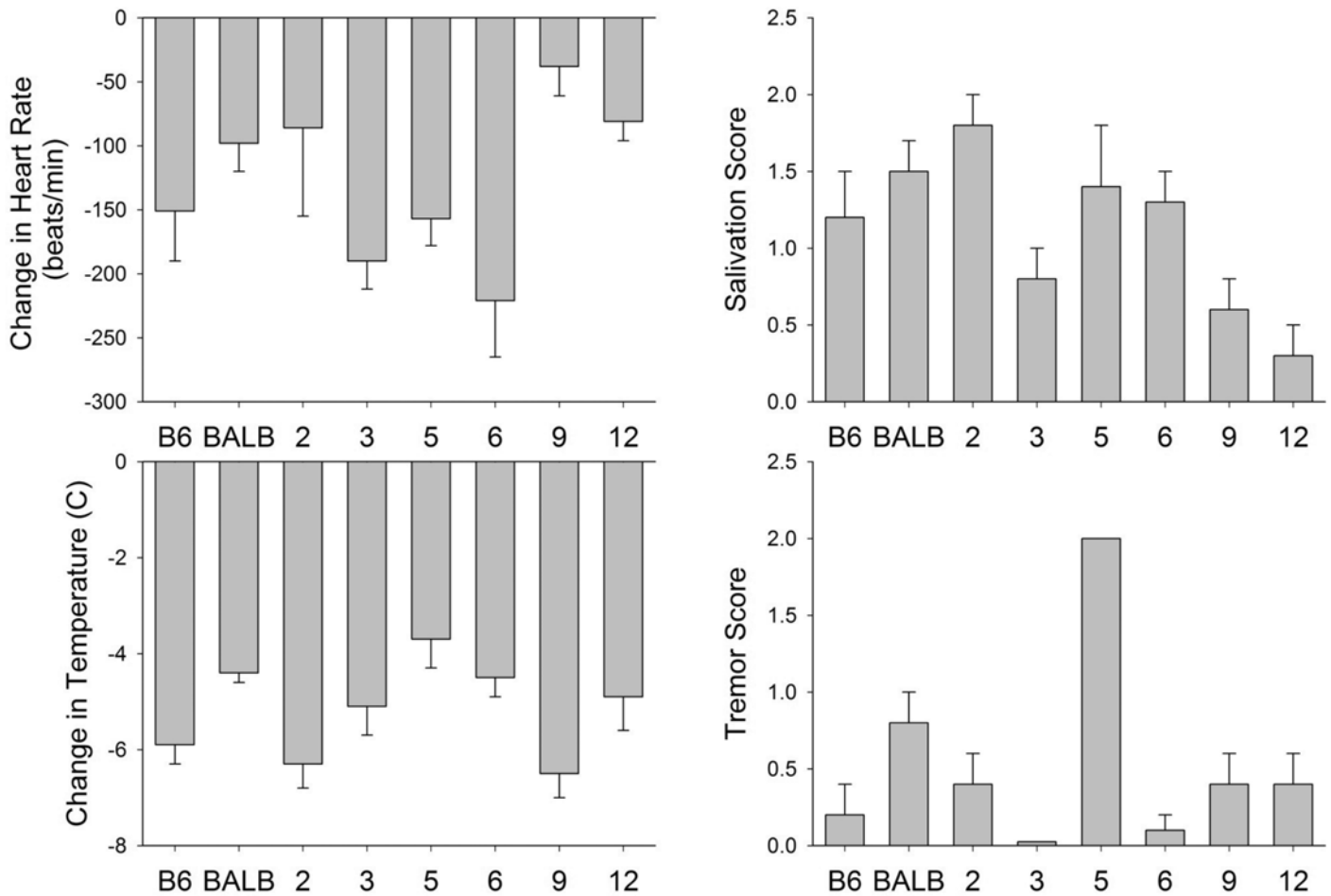


**Figure 3.** Physiologic and behavioral responses to oxotremorine in C57BL/6J, BALB/cByJ, and CXB recombinant inbred mice. Body temperature, heart rate, and salivation were assessed at 30 min after intraperitoneal injection of 0.1 mg/kg oxotremorine (C57BL/6J,  $n = 6$ ; BALB/cByJ,  $n = 6$ ; CXB2,  $n = 5$ ; CXB3,  $n = 6$ ; CXB5,  $n = 5$ ; CXB6,  $n = 10$ ; CXB9,  $n = 10$ ; CXB12,  $n = 7$ ). Tremor was assessed as: 0, no tremor; 1, intermittent head and body tremor; or 2, nearly continuous whole-body tremor. Salivation was assessed as: 0, none; 1, mild; 2, moderate; or 3, severe. For all panels, data are presented as mean  $\pm$  SEM (bars).

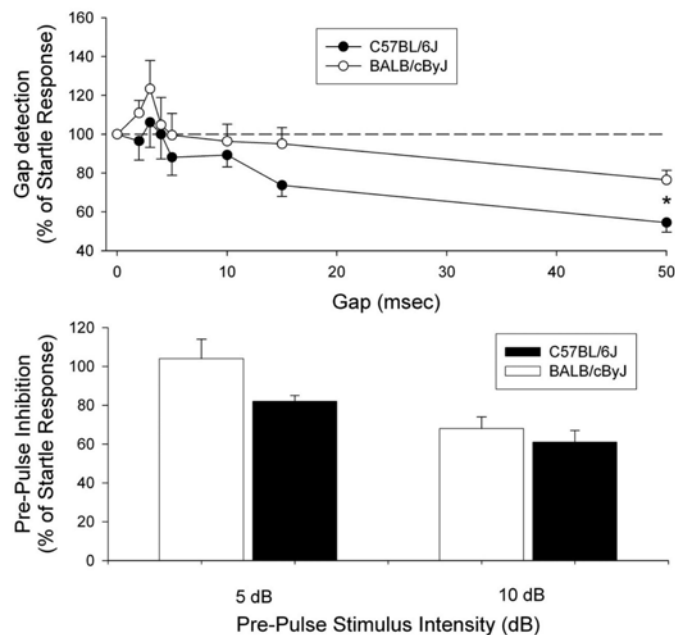
circuit contains additional structural elements.<sup>20,38</sup> With regard to startle, auditory signals pass through the cochlear nucleus and the giant neurons of the pontine reticular nucleus before impacting the motor neurons.<sup>20</sup> In contrast, auditory signals responsible for PPI pass to the pontine reticular nucleus through the inferior colliculus, the forebrain, and other structures. The pontine reticular nucleus, which contains abundant inhibitory muscarinic receptors, is widely viewed as the sensorimotor interface for startle and PPI. Therefore, within the pontine reticular nucleus, information about prepulse stimuli and other relevant cues converges with the startle stimulus; the output of the pontine reticular nucleus is then directed to the spinal motor neurons to produce the startle reflex.<sup>3</sup> The muscarinic receptors in the pontine reticular nucleus have a prominent role in modulating startle and its inhibition by prepulse stimuli.<sup>2</sup> Acetylcholine acts on M1R and M2R in the principal sensory trigeminal nucleus of rats and mice to contribute to selective gating of ascending sensory transmission.<sup>16</sup>

Various strains of inbred mice differ substantially in sensorimotor gating, as behaviorally identified by measuring PPI.<sup>38</sup> Consistent with a previous report,<sup>1</sup> we observed less PPI in BALB/cByJ mice than in C57BL/6J mice, as well as greater startle am-

plitude in BALB/cByJ mice as compared with C57BL/6J mice. These characteristics could reflect a higher basal state of arousal in BALB/cByJ mice. However, BALB/c mice also experience significant age-related hearing loss that develops earlier than in C57BL/6 mice,<sup>38</sup> and hearing loss has been associated with greater startle amplitude as long as the frequency characteristics of the startle stimulus are in the still-audible range of hearing.<sup>12</sup> In addition, the greater gap detection and PPI of C57BL/6J compared with BALB/cByJ mice potentially are related to poor hearing in the latter strain. The greater PPI of the CXB6 strain suggests better hearing or sensory gating in that strain as compared with the others. Similarly, less and greater startle, as seen in CXB6 and CXB12 compared with CXB3 and CXB9 strains, suggests less and greater tonic inhibition of the startle reflex, respectively. Therefore, these strain differences could be related to differences in either baseline arousal or hearing, with relatively lower inhibitory muscarinic tone associated with relatively greater startle. However, we were unable to demonstrate association between these responses and the *Chrm2* mutation. The significant strain  $\times$  PPI intensity interaction appeared to be driven by the inverse pattern of responding as a function of prepulse intensity in CXB3 and CXB6 strains.

**Table 1.** *Chrm2* genotype and phenotype strain distribution patterns

Strain	<i>Chrm2</i> genotype <sup>a</sup>	Startle amplitude <sup>b</sup>	PPI <sup>c</sup>	Responses at 30 min after injection of 0.1 mg.kg oxotremorine			
				Hypothermia (°C)	Tremor <sup>d</sup>	Salivation <sup>d</sup>	Bradycardia (bpm) <sup>d</sup>
BALB/cByJ	BALB/cByJ	high	impaired	-4.4 ± 0.4	1.5 ± 0.2	1.5 ± 0.2	-98 ± 22
C57BL/6J	C57BL/6J	low	normal	-4.0 ± 0.6	1.8 ± 0.2	1.2 ± 0.3	-151 ± 39
CXB2	C57BL/6J	not tested	not tested	-6.3 ± 0.5	1.8 ± 0.2	1.8 ± 0.2	-86 ± 69
CXB3	BALB/cByJ	low	impaired	-5.1 ± 0.6	2.0 ± 0.4	0.8 ± 0.2	-190 ± 22
CXB5	BALB/cByJ	not tested	not tested	-3.7 ± 0.6	2.0 ± 0.3	1.4 ± 0.4	-157 ± 21
CXB6	BALB/cByJ	high	normal	-4.5 ± 0.4	1.9 ± 0.1	1.3 ± 0.2	-221 ± 44
CXB9	BALB/cByJ	low	impaired	-6.5 ± 0.5	0.7 ± 0.2	0.6 ± 0.2	-38 ± 23
CXB12	C57BL/6J	high	impaired	-4.9 ± 0.7	1.8 ± 0.2	0.3 ± 0.2	-81 ± 15

<sup>a</sup>Data from Figure 1<sup>b</sup>Data from Figures 4,5; relative amplitudes<sup>c</sup>Data from Figures 4,5 (10 dB)<sup>d</sup>Data from Figures 2,3

**Figure 4.** Gap detection and prepulse inhibition in C57BL/6J and BALB/cByJ mice. In the top panel, baseline and startle amplitudes were collected in the presence of a 60-dB SPL broadband background noise. Baseline values provide an estimate of the force applied to the testing plate when the mouse is ambulating, grooming, and so forth (that is, not during the startle stimulus). Startle stimuli consisted of 110-dB SPL, 20-ms noise bursts. The responses to gaps were measured by comparing trials with a startle-only stimulus and trials consisting of the same startle stimulus preceded by a silent gap in the background noise. During the gap, the 60-dB background noise was turned off. Gap duration varied from 0 ms (startle-only trials) to 50 ms, and the beginning of the gap was always 100 ms before the presentation of the startle stimulus. Overall gap detection was not significantly different between C57BL/6J and BALB/cByJ mice ( $n = 10$  per strain). In the bottom panel, prepulse inhibition (PPI) was determined by using stimuli of either 5 or 10 dB above the background noise (65 or 70 dB). Stimuli were 50 ms in duration and always began 100 ms before the presentation of the startle stimulus. PPI differed significantly ( $P = 0.002$ ) between strains at 10 dB above background. For both panels, data are presented as mean  $\pm$  SEM (bars).

Among the phenotypic differences examined here, none corresponds reliably with the specific *Chrm2* genotype across several strains of CXB RI mice (Table 1). This lack of association indicates that the *Chrm2* genotype is not a major factor in mediating expression of these phenotypes. However, several caveats prevent the broad conclusion that this mutation does not encode a phenotype. First, our primary comparisons were of 2 inbred strains that differ widely according to analysis of single-nucleotide polymorphisms,<sup>26</sup> and numerous differences between these 2 strains are well established.<sup>25</sup> These major and fundamental strain differences may have masked or precluded detection of the phenotypic effect of a single point mutation. Second, the expression of a phenotype depends on the genetic background; some backgrounds may be permissive for expression of a phenotype, whereas others are not. More definitive demonstration of lack of a phenotype associated with *Chrm2* polymorphisms would require creating congenic strains of mice such that the C57BL/6J allele for *Chrm2* was present on the BALB/cByJ background, and vice versa. However, even this approach is not conclusive because congenic mice retain a genomic segment from the donor strain that encompasses the gene of interest and because the genomic backgrounds of either strain could mask phenotypes that might be apparent in other (that is, permissive) strains. Third, various physiologic and environmental factors can influence expression and detection of a phenotypic difference between mouse strains. Fourth, the phenotypes tested here represent only a subset of processes that are influenced by M2R. A different approach to testing the phenotypes we selected here or testing additional different CHRM2-associated processes (for example, using electrophysiologic patch-clamp approaches) potentially could reveal a discernable effect of the mutation. Such considerations reduce the likelihood of ever being able to entirely rule out the possibility that a genotype-phenotype relationship associated with a point mutation does not exist for any given process under some combination of genetic background, polymorphisms, physiologic state, and environment. Furthermore, our study reinforces the reality that despite the controlled environment and genetics of laboratory mice, associating complex phenotypes with a single gene is difficult. This complexity suggests caution in the interpretation of similar human studies seeking to identify single-gene effects on complex phenotypes, given that human studies generally are associated with far more genetic and environmental variability



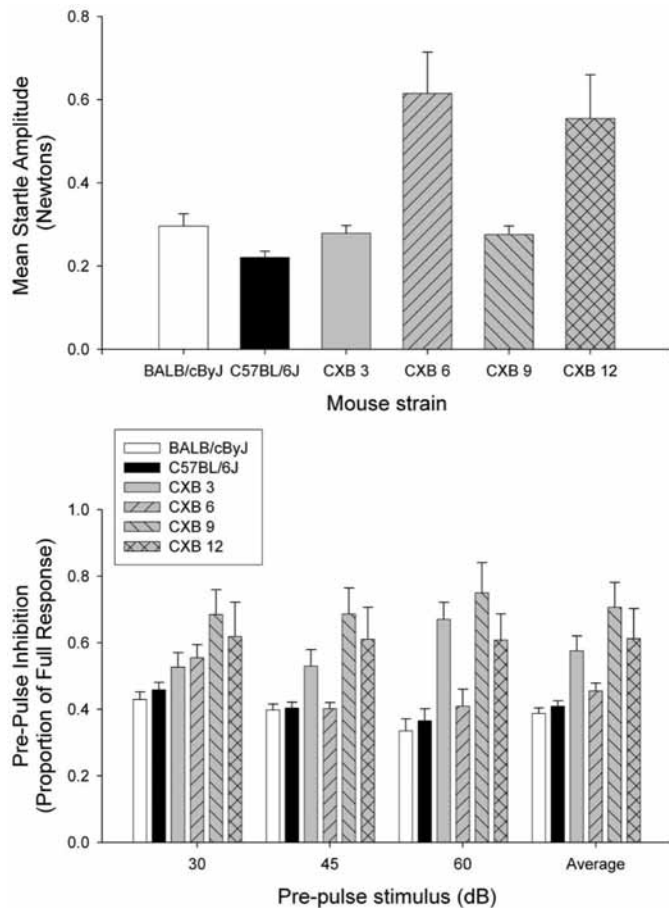


**Figure 5.** Prepulse inhibition in CXB recombinant inbred strains. In the top panel, startle amplitude was measured against a quiet background to avoid effects due to differences in hearing ( $n = 10$  per strain). Startle amplitude was significantly ( $P = 0.002$ ) different across RI strains. Error bars = standard error of the mean. In the bottom panel, recombinant inbred (RI) mice ( $n = 9$  or 10 per strain) were tested for prepulse inhibition (PPI) by using stimuli of 30, 45, and 60 dB instead of 5 or 10 dB above a 60-dB background, to allow more sensitive determination of whether differences in PPI were due to hearing loss or general deficits in sensory gating. PPI inhibition was significantly ( $P = 0.05$ ) different across the RI strains, and a significant ( $P = 0.002$ ) strain  $\times$  PPI intensity interaction was detected.

than are animal studies. Human studies manage this variability to some extent by using much larger sample sizes (for example,<sup>22</sup>).

In summary, we were unable to identify an association of the C797T→P266L *Chrm2* mutation with the phenotypes of receptor binding, *Chrm2* mRNA in acetylcholine-rich brain regions, behavioral responses to OXO, and measures of arousal and sensorimotor gating. However, the mutation nonetheless potentially could influence receptor binding or signal transduction properties in ways that were not tested in our study. In addition, a modulatory role that is perhaps influenced by other aspects of the genetic background, physiologic state, or environment, rather than an overt effect on general M2R function, remains possible for this polymorphism. Therefore, researchers who study CHRM2-related processes in mouse models should be aware of this mutation and consider its potential effect on experimental outcomes.

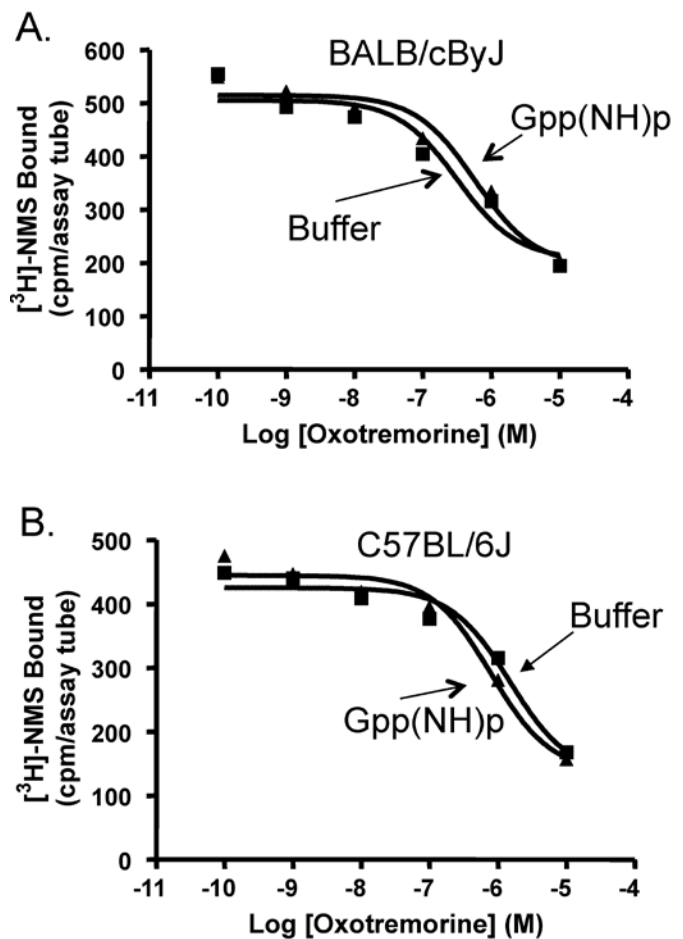


**Figure 6.** Influence of GTP $\gamma$ S on oxotremorine competition for [<sup>3</sup>H]NMS binding to heart homogenates. The ability of 10  $\mu$ M GTP $\gamma$ S to shift the oxotremorine competition curve was determined in heart homogenates from (A) BALB/cByJ mice and (B) C57BL/6J mice. GTP $\gamma$ S shifted the oxotremorine competition curve of BALB/cByJ mice but did not affect the curve of C57BL/6J mice.

### Acknowledgments

The authors thank Christine Bosgraaf, Lisa Cox, Rhett Gairani, Jennifer Parrish, Joshua Pikora, and Deb Larsen for providing technical assistance. This work was supported in part by NIH grants R01-NS40220 (LT), K26-RR17543 (LT), and R21-DC008357 (JT) and by the Southern Illinois University School of Medicine.

### References

1. Aubert L, Reiss D, Ouagazzal AM. 2006. Auditory and visual prepulse inhibition in mice: parametric analysis and strain comparisons. *Genes Brain Behav* 5:423–431.
2. Bosch D, Schmid S. 2006. Activation of muscarinic cholinergic receptors inhibits giant neurons in the caudal pontine reticular nucleus. *Eur J Neurosci* 24:1967–1975.
3. Carlson S, Willott JF. 1998. Caudal pontine reticular formation of C57BL/6J mice: responses to startle stimuli, inhibition by tones, and plasticity. *J Neurophysiol* 79:2603–2614.
4. Christopoulos A, Kenakin T. 2002. G protein-coupled receptor allostery and complexing. *Pharmacol Rev* 54:323–374.
5. Cohen-Woods S, Gaysina D, Craddock N, Farmer A, Gray J, Gunasinghe C, Hoda F, Jones L, Knight J, Korszun A, Owen MJ, Sterne A, Craig IW, McGuffin P. 2009. Depression Case Control (DeCC)

- Study fails to support involvement of the muscarinic acetylcholine receptor M2 (CHRM2) gene in recurrent major depressive disorder. *Hum Mol Genet* **18**:1504–1509.
6. **Comings DE, Wu S, Rosthamkhani M, McGue M, Iacono WG, MacMurray JP.** 2002. Association of the muscarinic cholinergic 2 receptor (CHRM2) gene with major depression in women. *Am J Med Genet* **114**:527–529.
  7. **Ding M, Lu L, Toth LA.** 2008. Gene expression in lung and basal forebrain during influenza infection in mice. *Genes Brain Behav* **7**:173–183.
  8. **Greenwood PM, Lin MK, Sundararajan R, Fryxell KJ, Parasuraman R.** 2009. Synergistic effects of genetic variation in nicotinic and muscarinic receptors on visual attention but not working memory. *Proc Natl Acad Sci USA* **106**:3633–3638.
  9. **Gritti I, Mainville L, Jones BE.** 1993. Codistribution of GABA with acetylcholine-synthesizing neurons in the basal forebrain of the rat. *J Comp Neurol* **329**:438–457.
  10. **Hautala AJ, Tulppo MP, Kiviniemi AM, Rankinen T, Bouchard C, Makikallio TH, Huikuri HV.** 2009. Acetylcholine receptor M2 gene variants, heart rate recovery, and risk of cardiac death after an acute myocardial infarction. *Ann Med* **41**:197–207.
  11. **Ichiyama S, Oka Y, Haga K, Kojima S, Taisi Y, Shirakawa M, Haga T.** 2006. The structure of the third intracellular loop of the muscarinic acetylcholine receptor M2 subtype. *FEBS Lett* **580**:23–26.
  12. **Ison JR, Allen PD, O'Neill WE.** 2007. Age-related hearing loss in C57BL/6J mice has both frequency-specific and non-frequency specific components that produce a hyperacusis-like exaggeration of acoustic startle. *J Assoc Res Otolaryngol* **8**:539–550.
  13. **Jacoby DB, Xiao HQ, Lee NH, Chan-Li Y, Fryer AD.** 1998. Virus- and interferon-induced loss of inhibitory M2 muscarinic receptor function and gene expression in cultured airway parasympathetic neurons. *J Clin Invest* **102**:242–248.
  14. **Jones BE.** 2000. Basic mechanisms of sleep–wake states, p 134–154. In: Kryger MH, Roth T, Dement WC, editors. *Principles and practice of sleep medicine*. New York (NY): WB Saunders.
  15. **Jones KA, Porjesz B, Almasy L, Bierut L, Dick D, Goate A, Hinrichs A, Rice JP, Wang JC, Bauer LO, Crowe R, Foroud T, Hesselbrock V, Kuperman S, Nurnberger J, O'Connor SJ, Rohrbach J, Schuckit MA, Yischfield J, Edenberg HJ, Begleiter H.** 2006. A cholinergic receptor gene (CHRM2) affects event-related oscillations. *Behav Genet* **36**:627–639.
  16. **Kohlmeier KA, Soja PJ, Kristensen MP.** 2006. Disparate cholinergic currents in rat principal trigeminal sensory nucleus neurons mediated by M1 and M2 receptors: a possible mechanism for selective gating of afferent sensory neurotransmission. *Eur J Neurosci* **23**:3245–3258.
  17. **Krejci A, Michal P, Jakubik J, Ricny J, Dolezal V.** 2004. Regulation of signal transduction at M2 muscarinic receptor. *Physiol Res* **53 Suppl. 1**:S131–S140.
  18. **Larcombe AN, Zosky GR, Bozanich E, Turner DJ, Hantos A, Sly PD.** 2008. Absence of cholinergic airway tone in normal BALB/c mice. *Respir Physiol Neurobiol* **161**:223–229.
  19. **Levey AI, Edmunds SM, Hersch SM, Wiley RG, Hellman CJ.** 1995. Light and electron microscopic study of m2 muscarinic acetylcholine receptor in the basal forebrain of the rat. *J Comp Neurol* **351**:339–356.
  20. **Lingenhohl K, Friauf E.** 1994. Giant neurons in the rat reticular formation: a sensorimotor interface in the elementary acoustic startle reflex circuit? *J Neurosci* **14**:1176–1194.
  21. **Mistry R, Dowling MR, Challiss RA.** 2005. An investigation of whether agonist-selective receptor conformations occur with respect to M2 and M4 muscarinic acetylcholine receptor signaling via Gi/o and Gs proteins. *Br J Pharmacol* **144**:566–575.
  22. **Mobascher A, Rujescu D, Mittelstrass K, Giegling I, Lamina C, Nitz B, Brenner H, Fahr C, Breitling LP, Gallinat J, Rothenbacher D, Raum E, Muller H, Ruppert A, Hartmann AM, Moller HJ, Gal A, Gieger C, Wichmann HE, Illig T, Dahmen N, Winterer G.** 2009. Association of a variant in the muscarinic acetylcholine receptor 2 gene (*CHRM2*) with nicotine addiction. *Am J Med Genet B Neuropsychiatr Genet* **153B**:684–690.
  23. **Nelson CP, Nahorski SR, Chaliss RA.** 2006. Constitutive activity and inverse agonism at the M2 muscarinic acetylcholine receptor. *J Pharmacol Exp Ther* **16**:279–288.
  24. **Paxinos G, Franklin KBJ.** 2001. *The mouse brain in stereotaxic coordinates*. New York (NY): Academic Press.
  25. **Paylor R, Crawley JN.** 1997. Inbred strain differences in prepulse inhibition of the mouse startle response. *Psychopharmacology (Berl)* **132**:169–180.
  26. **Petkov PM, Ding Y, Cassell MA, Zhang W, Wagner G, Sargent EE, Asquith S, Crew V, Johnson KA, Robinson P, Scott VE, Wiles MV.** 2004. An efficient SNP system for mouse genome scanning and elucidating strain relationships. *Genome Res* **14**:1806–1811.
  27. **Proskosil BJ, Fryer AD.** 2005. Beta2-agonist and anticholinergic drugs in the treatment of lung disease. *Proc Am Thorac Soc* **2**:305–310.
  28. **Semba K.** 2000. Multiple output pathways of the basal forebrain: organization, chemical heterogeneity, and roles in vigilance. *Behav Brain Res* **115**:117–141.
  29. **Swerdlow NR, Braff DL, Geyer MA.** 1999. Cross-species studies of sensorimotor gating of the startle reflex. *Ann N Y Acad Sci* **877**:202–216.
  30. **Szczepankiewicz A, Breborowicz A, Sobkowiak P, Kramer L, Popiel A.** 2009. Association of A/T polymorphism of the CHRM2 gene with bronchodilator response to ipratropium bromide in asthmatic children. *Pneumonol Alergol Pol* **77**:5–10.
  31. **Tayebati SK, Piergentili A, Natale D, Amenta F.** 1999. Evaluation of an agonist index: affinity ratio for compounds active on muscarinic cholinergic M2 receptors. *J Auton Pharmacol* **19**:77–84.
  32. **Toth LA.** 1996. Strain differences in the somnogenic effects of interferon inducers in mice. *J Interferon Cytokine Res* **16**:1065–1072.
  33. **Toth LA, Rehg JE, Webster RG.** 1995. Strain differences in sleep and other pathophysiological sequelae of influenza virus infection in naive and immunized mice. *J Neuroimmunol* **58**:89–99.
  34. **Toth LA, Williams RW.** 1999. A quantitative genetic analysis of slow-wave sleep in influenza-infected CXB recombinant inbred mice. *Behav Genet* **29**:339–348.
  35. **Wang GY, Lee CG, Lee EJ.** 2004. Genetic variability of arylalkylamine-N-acetyl-transferase (AA-NAT) gene and human sleep/wake pattern. *Chronobiol Int* **21**:229–237.
  36. **Wess J.** 2004. Muscarinic acetylcholine receptor knockout mice: novel phenotypes and clinical implications. *Annu Rev Pharmacol Toxicol* **44**:423–450.
  37. **Willott JF, Tanner L, O'Steen J, Johnson KR, Bogue MA, Gagnon L.** 2003. Acoustic startle and prepulse inhibition in 40 inbred strains of mice. *Behav Neurosci* **117**:716–727.
  38. **Willott JF, Turner JG, Carlson S, Ding D, Seegers-Bross L, Falls WA.** 1998. The BALB/c mouse as an animal model for progressive sensorineural hearing loss. *Hear Res* **115**:162–174.
  39. **Wills-Karp M, Luyimbazi J, Xu X, Schofield B, Neben TY, Karp CL, Donaldson DD.** 1999. Interleukin-13: central mediator of allergic asthma. *Science* **282**:2258–2261.
  40. **Young JS, Fletcher LD.** 1983. Reflex inhibition procedures for animal audiometry: a technique for assessing ototoxicity. *J Acoust Soc Am* **73**:1686–1693.